MproTAC - New approach for development of SARS-CoV-2 antiviral drugs

Kaixuan Zhang[1], Judith Röske[1], Lisa Buddrus[1], Hannah Maple[2], Alex Moloney[2], Graham Marsh[2], Mark Cooper[2], Burhan Karadogan[2], You-Ting Chen[3], Katharina Rox[3], Mark Brönstrup[3,4], Arne Meyer[5], Melissa Graewert[6], Rolf Hilgenfeld[1,4]

1 University of Lübeck, Institute of Molecular Medicine, Lübeck, Germany; 2 Bio-techne, Bristol, United Kingdom; 3 Helmholtz-Centre for Infection Research, Braunschweig;

4 German Center for Infection Research (DZIF), Germany; 5 XtalConcepts GmbH, Hamburg, Germany; 6 European Molecular Biology Laboratory c/o DESY, Hamburg, Germany

Introduction

Following the outbreak of COVID-19, many direct-acting antiviral therapies have been developed [1]. A number of drugs (nirmatrelvir, ensitrelvir) have been approved as inhibitors of the SARS-CoV-2 main protease (Mpro). An alternative approach has recently been introduced with the Proteolysis-Targeting Chimeras (PROTACs).

PROTACs [2] are hetero bifunctional molecules that stimulate ubiquitin transfer to attain target protein degradation. They are composed of the protein of interest (POI) ligand and an E3 recruiting ligand connected by a linker. Different from the competitive and occupancy-driven mode of action (MOA) of inhibitors, PROTACs recruit E3 ligase to the POI and induce the ubiquitin-proteasome-system [3] (UPS) via the 26S proteasome. The result will be the degradation of the POI. Due to the catalytic event-driven MOA, degraders could achieve efficacy in lower doses as compared to conventional inhibitors, thus minimizing potential toxicity and side-effects. We have currently some lead MproTACs (Mpro PROTACs) that recruit SARS-CoV-2 Mpro. We characterized them by using biochemical and biophysical techniques. Here, we present our work on the shape and dynamics of ternary complexes involving Mpro, a chemical linker, and DDB1- CRBN (the ubiquitin ligase) / CRBN midi.

Figure 1. PROTAC concept: Direct recruitment of an E3 ligase by using the PROTAC

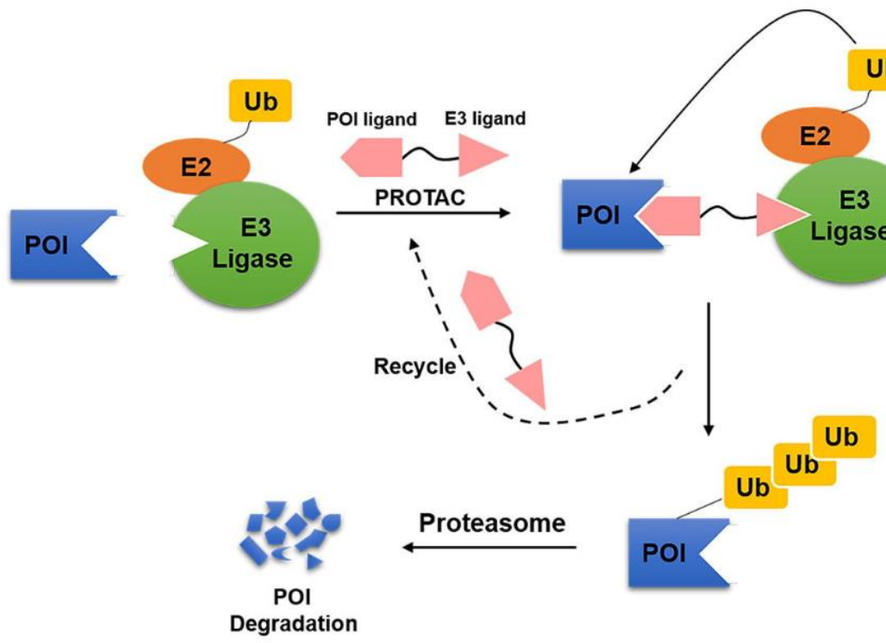

Image from: J.Y Xi et al. *J. Bioorg*. 2022,105848, Advances and perspectives of proteolysis targeting chimeras (PROTACs) in drug discovery.

Figure 2. Structure of MproTACs with non-covalent C10778 and covalent 13b-K Mpro ligands

Name	Mpro ligand type	Structure
C10778N Designed after Mpro Inhibitor compound 19 [4]	non-covalent	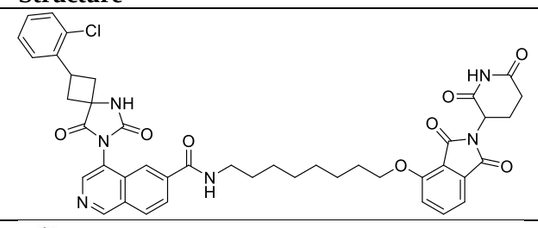
BT153 From series 13b-K [5]	covalent	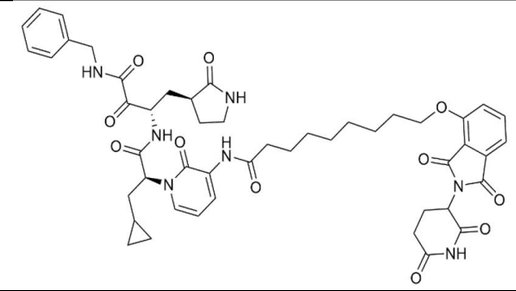

Chemical structures of Mpro ligands used in this study include the non-covalent (Compound 19 [4]) and covalent (13b-K [5]) inhibitors.

Figure 3a. Inhibition of Mpro by PROTACs

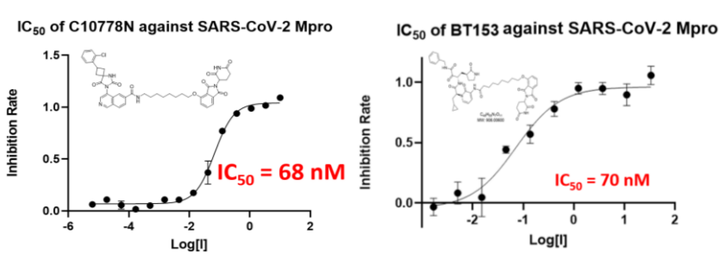

Determination of inhibition (IC_{50}) by using a fluorescent substrate with the cleavage site (indicated by the arrow, ↓) of SARS-CoV-2 Mpro (Dabcyl-KTSAVLQ↓SGFRKM-E (Edans)-NH_2).

Figure 3b. Antiviral activity (EC_{50}) of MproTACs

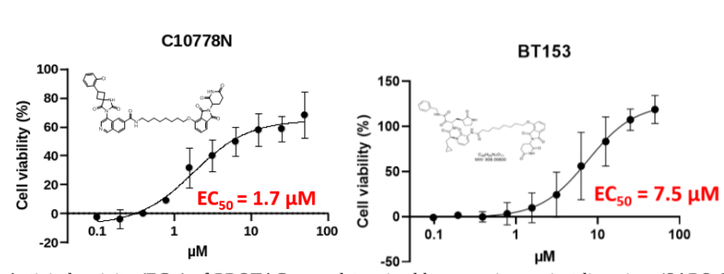

Antiviral activity (EC_{50}) of PROTACs was determined by screening against live virus (SARS-CoV-2/ZG/297–20, MOI 0.05) in Vero E6 cells using a cell viability assay (CellTiter-Glo®).

Figure 4. Surface plasmon resonance (SPR) to determine MproTAC binding affinity

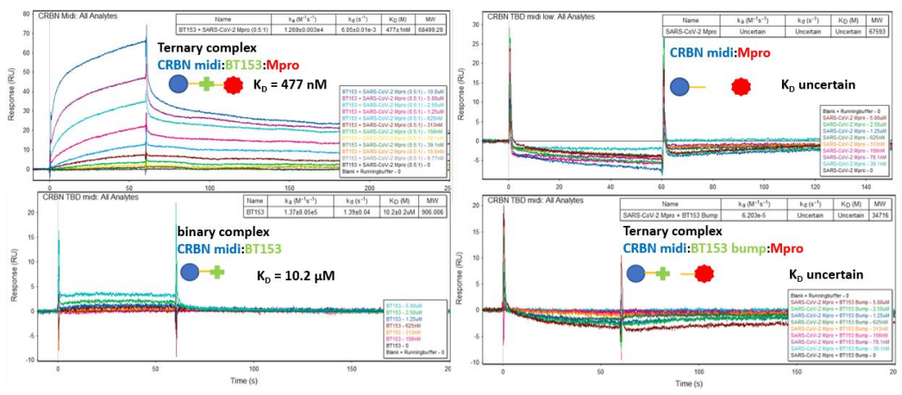

CRBN midi [6] (hCRBN_UniProt: Q96SW2, residue 41-187 and residue 249-426 connected by a GSG loop) was immobilized on a Hiscap chip to determine the K_D value using the Octet® SPR instrument from Sartorius. BT153 bump served as a negative control. (binding to Mpro but not to CRBN midi)

Figure 5. Dynamic Light-Scattering (DLS) to determine ternary complex formation

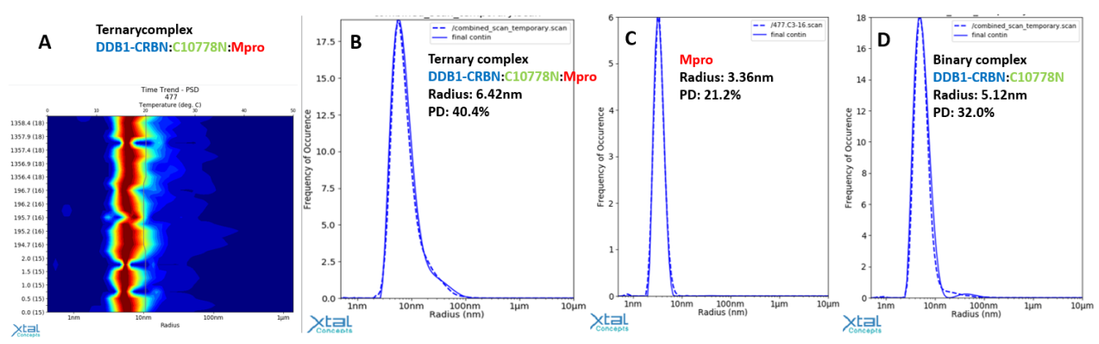

Determination of protein size in solution (DLS) by using the instrument SpectroLight 600 from XtalConcepts GmbH, Hamburg. **A** describes the level of protein aggregation by size (radius) and time trend (unit / min). **B**-**D** show the size of the protein (radius) by peak and the polydispersity (PD) index.

Figure 6. Small-angle X-ray-scattering to derive low-resolution structure of ternary complex

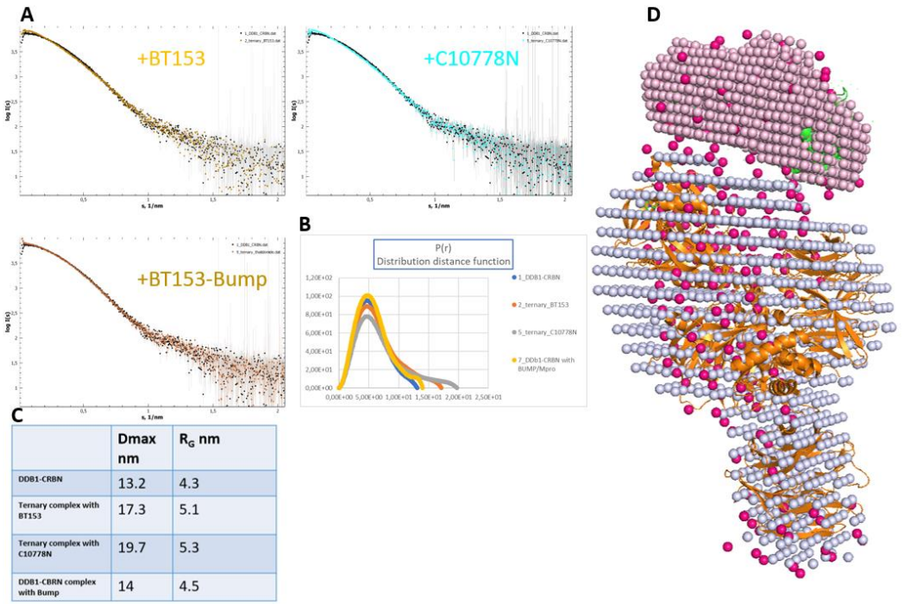

	Dmax nm	R_G nm
DDB1-CRBN	13.2	4.3
Ternary complex with BT153	17.3	5.1
Ternary complex with C10778N	19.7	5.3
DDB1-CRBN complex with Bump	14	4.5

Biological Small-angle X-ray scattering data of MproTACs BT153 and C10778N. **A.** Scattering curves I(*S*) for ternary complex of BT153, C10778N and BT153 bump (negative control). (I, intensity of scattering) as a function of momentum transfer ($s = 4\pi\sin(\theta)/\lambda$) and is displaced along the y-axis for visualization. **B.** Normalized pair distance distribution functions P(r) calculated from the scattering profiles by PRIMUS for DDB1-CRBN (blue), ternary_BT153 (orange), ternary_C10778N (grey), DDB1-CRBN with BT153bump (yellow). **C.** Summary data of Dmax (the maximum size of protein molecule) and R_G (radius of gyration). The comparison shows ternary complex formation with BT153 and C10778N. **D.** Ab initio models built by DAMMIF with the fit of the SAXS envelope to the corresponding high-resolution structure. DDB1-CRBN (orange, PDB 8oiz) and SARS-CoV-2 Mpro (green, PDB 6y2e) were superimposed on to the SAXS model. The experiment was conducted at the EMBL beamline P12 (Petra III, DESY, Hamburg).

References

[1] G. Li, R. Hilgenfeld, R. Whitley & E. De Clercq. *Nat. Rev. Drug. Discov. 2023*, 22, 449-475.
[2] D. L. Buckley, C. M. Crews, *Angew. Chem. Int. Ed. 2014*, 53, 2312-2330.
[3] A. Ciechanover, A. L. Schwartz. *Proc Natl. Acad. Sci. USA 1998*, 95, 2727-2730.
[4] A. Luttens et al. *J. Am. Chem. Soc. 2022*, 144, 2905-2920.
[5] M. S. Cooper et al. *J. Med. Chem. 2022*, 65, 13328-13342.
[6] D. Zollman, A. Ciulli et al. *bioRxiv. 2024*, https://doi.org/10.1101/2024.01.17.575503.